

Quark masses and strong coupling constant in 2+1 flavor QCD

Y. Maezawa^a and P. Petreczky^b,

^a *Yukawa Institute for Theoretical Physics, Kyoto University, Kyoto 606-8317, Japan*

^b *Physics Department, Brookhaven National Laboratory, Upton, New York 11973, USA*

(Dated: September 6, 2016)

We present a determination of the strange, charm and bottom quark masses as well as the strong coupling constant in 2+1 flavor lattice QCD simulations using highly improved staggered quark action. The ratios of the charm quark mass to the strange quark mass and the bottom quark mass to the charm quark mass are obtained from the meson masses calculated on the lattice and found to be $m_c/m_s = 11.877(91)$ and $m_b/m_c = 4.528(57)$ in the continuum limit. We also determine the strong coupling constant and the charm quark mass using the moments of pseudoscalar charmonium correlators: $\alpha_s(\mu = m_c) = 0.3697(85)$ and $m_c(\mu = m_c) = 1.267(12)$ GeV. Our result for α_s corresponds to the determination of the strong coupling constant at the lowest energy scale so far and is translated to the value $\alpha_s(\mu = M_Z, n_f = 5) = 0.11622(84)$.

PACS numbers: 12.38. Gc, 12.38.-t, 12.38.Bx

I. INTRODUCTION

Accurate determination of QCD parameters received a lot of attention in recent years. Lattice QCD calculations play an important role in this quest. The precise knowledge of the QCD parameters is important for testing the prediction of the standard model. One prominent example is the sensitivity of Higgs branching ratios to the heavy quark masses and the strong coupling constant [1]. While several precise determinations of the heavy quark masses and the strong coupling constant α_s on the lattice exist, it is always important to obtain results using different lattice methods to ensure that all the errors are under control. In the case of α_s different lattice and nonlattice methods often give quite different results, possibly suggesting that not all the sources of errors are under control [2]. In particular, the lattice determinations that use the static quark antiquark potential lead to smaller values of α_s [3, 4]. As a result of this the error on the α_s quoted in the most recent Particle Data Group (PDG) Review update has increased for the first time in many years: $\alpha_s(M_Z) = 0.1181(16)$ [5]. This should be compared to the 2013 PDG value, $\alpha_s(M_Z) = 0.1185(6)$. Lattice QCD offers the possibility to determine the strong coupling constant at relatively low energy scales. So far the only nonlattice method that offers a low energy determination of α_s is the analysis of the τ decay but there are large systematic uncertainties due to different ways of organizing the perturbative expansion in this method (see Ref. [6] for a recent work on this topic and references therein). For certain applications it is important to have the running of the coupling constant at low energy scales. One example is the comparison of weak coupling and lattice results in QCD thermodynamics, where the typical scale $\approx \pi T$ could be as low as 1 GeV [7–10].

There are also sizable differences in the value of the charm quark masses. The recent determination of m_c by the HPQCD Collaboration [11] is significantly lower than the value obtained by the ETMC Collaboration [12]. Some lattice QCD calculations use 2 or 3 flavors of dynamical quarks [13–15], while others use 4 dynamical flavors [11, 12, 16]. Therefore, understanding of the flavor dependence of the charm quark mass is also important.

Furthermore, nonperturbative determination of the bottom quark mass is a problematic matter in the lattice simulations due to the discretization errors caused by powers of $m_h a$, where m_h is the bare mass of the heavy quarks. However, owing to improvements of discretization of the action as well as simulations with smaller lattice spacing using powerful computing resources, it has recently become possible to perform calculations with quark masses larger than the charm quark mass. The region around the bottom quark mass can be accessed using extrapolations [17]. Several determinations of the quark mass ratio of the bottom to charm have been reported, and a slight inconsistency has been found: The ratio recently obtained by the ETMC Collaboration [18] shows smaller value than that previously determined by the HPQCD Collaborations [11, 17]. Thus the determinations of the bottom quark mass with different setups and approaches are also important to provide precise theoretical predictions.

In this paper we report on the calculation of the quark masses and the strong coupling constant in 2+1 flavor QCD using highly improved staggered quark (HISQ) action. More precisely, we determine the ratio of the charm quark mass to the strange quark mass and the bottom quark mass to the charm quark mass from the pseudoscalar and vector meson masses calculated on the lattice and combined with the experimental inputs. Furthermore, the strong coupling constant α_s and the charm quark mass $m_c(m_c)$ in $\overline{\text{MS}}$ renormalization scheme are determined from the moments of the pseudoscalar charmonium correlators and the comparison to the corresponding perturbative result. By using the quark mass ratios together with α_s and $m_c(m_c)$, we also determine the strange and bottom quark masses.

This paper is organized as follows: In Sec. II we introduce the details of the lattice setup and explain our approach to determine the quark mass ratios, the strong coupling constant and the quark masses. Our main numerical results are discussed in Sec. III, including the determination of the physical values of the charm quark mass and the ratios of the quark masses, as well as the moments of the pseudoscalar charmonium correlators. In Sec. IV we compare our results for the strong coupling constant and the quark masses with other lattice results. The paper is concluded in Sec. V.

II. LATTICE SETUP AND DETAILS OF ANALYSIS

To determine the quark masses and the strong coupling constant, we calculate meson masses as well as the moments of pseudoscalar charmonium correlators in 2+1 flavor lattice QCD. The gauge configuration used in our study has been generated using tree-level improved gauge action [19] and highly improved staggered quark (HISQ) action [20] by the HotQCD Collaboration [21]. The strange quark mass, m_s , was fixed to its physical value, while for the light (u and d) quark masses the value $m_l = m_s/20$ was used. The later corresponds to the pion mass of 160 MeV in the continuum limit. Thus, the values of the light quark masses are slightly larger than the physical value. This small difference, however, does not lead to any visible effects in the physical observables at zero temperature, which agree well with the experimental values [21, 22]. For the valence charm and bottom quarks we use the HISQ action with the so-called ϵ -term [20], which removes the tree-level discretization effects due to the large quark mass up to $O((am)^4)$. The HISQ action with ϵ -term turned out to be very effective for treating the charm quark on the lattice [16, 20, 22, 23]. The lattice spacing in our calculations has been fixed using the r_1 scale defined in terms of the energy of static quark antiquark pair $V(r)$ as

$$r^2 \frac{dV}{dr} \Big|_{r=r_1} = 1.0. \quad (1)$$

We use the value of r_1 determined in Ref. [24] using the pion decay constant as an input:

$$r_1 = 0.3106(18) \text{ fm}. \quad (2)$$

In the above equation all the sources of errors in Ref. [24] have been added in quadrature. The above value of r_1 corresponds to the value of the scale parameter determined from the Wilson flow $w_0 = 0.1749(14)$ [21]. This agrees very well with determination of the Wilson flow parameter by the BMW Collaboration, $w_0 = 0.1755(18)(4)$ [25]. It is also consistent with the HPQCD value $r_1 = 0.3133(23)(3)$ within errors [26]. This gives us confidence in our scale setting.

All of the quantities in this paper can be calculated from the meson correlation functions. In this study, we focus only on the local meson operators which have the same structures in the taste and spin generators of Dirac gamma matrices Γ . In particular, we calculate the meson propagators consisting of the pseudoscalar $\Gamma = \gamma_5$ and vector γ_i operators. To obtain the moments of the charmonium correlators (explained in detail below), we calculate the pseudoscalar meson correlators with the point sources. On the other hand, to determine the bare charm quark mass and quark mass ratios, m_c/m_s and m_b/m_c , we utilize the meson correlators obtained with the corner-wall sources, where on a given time slice we set the sources to one at the origin of each 2^3 cube and to zero elsewhere. The corner-wall sources enable reduction of the contribution of higher excited states and thus more accurate determination of the ground state masses. From the meson propagators, we extract the charmonium and bottomonium masses using two type of fits. The first type of fits includes only the ground

state contributions, while the second type of fits includes the ground state contribution and the first excited state contribution [27]. The second type of fit allows us to use a larger range in the time direction. We find that the two fits agree quite well. We also checked the fit range dependence of the extracted masses and found it to be small. Any dependence on the fit range that is larger than the statistical error is treated as a systematic error. For the determination of the ratio m_c/m_s , we need the mass of the unmixed pseudoscalar $s\bar{s}$ meson mass at the physical point and utilize the lattice results from Ref. [21].

Using the J/ψ and η_c masses obtained for several trial values of the lattice bare quark mass m_{ct} , we study the charm quark mass dependence of the spin averaged mass

$$\overline{M} = \frac{1}{4}(3M_{J/\psi} + M_{\eta_c}). \quad (3)$$

Using \overline{M} has the advantage that effects of hyperfine splitting, which are sensitive to discretization errors, cancel out in this combination. We fit the m_{ct} dependence of \overline{M} using the linear form

$$\overline{M} = d + bm_{ct}, \quad (4)$$

which works very well. Then the physical value of the bare charm quark mass can be determined as

$$m_{c0} = \frac{1}{b} \left[\overline{M} - d_0 \left(\frac{r_1}{a} \right) r_1^{-1} \right], \quad (5)$$

where we explicitly expressed d in terms of a dimensionless quantity given in the lattice unit: $d_0 = ad$.

The mass of the unmixed pseudoscalar meson is given by $M_{\eta_{ss}}^2 = Bm_{s0}$. Then, the mass ratio of the charm to strange quarks can be written as

$$\frac{m_{c0}}{m_{s0}} = \frac{B}{M_{\eta_{ss}}^2} \frac{\overline{M} - d}{b}. \quad (6)$$

By using the r_1 scale as well as the values of B , r_1/a , d_0 , and b , extracted on the lattice, the above equation can be rewritten as

$$\frac{m_{c0}}{m_{s0}} = \frac{B_0}{bM_{\eta_{ss}}r_1} \left(\frac{r_1}{a} \right) \left[\frac{\overline{M}}{M_{\eta_{ss}}} - \left(\frac{r_1}{a} \right) \frac{d_0}{M_{\eta_{ss}}r_1} \right], \quad (7)$$

where $B_0 = aB$. Since the ratio of the quark masses is scheme and scale independent, $m_c/m_s = m_{c0}/m_{s0}$, the above equation is the basis for our extraction of m_c/m_s . Using the experimental input for the meson masses \overline{M} and $M_{\eta_{ss}}$ on one hand and the value of the fit parameters b and d_0 obtained on the lattice together with the values of B_0 and r_1/a from Ref. [21] on the other hand, we can obtain the value of m_c/m_s at each lattice spacing. Next, we have to perform the continuum extrapolation of this ratio to obtain its physical value. In the next section, we discuss the numerical details of these steps along the discussion of the corresponding error budget.

A similar approach can be applied to the bottom quark mass and the ratio of the bottom to charm quark mass. With the meson correlation functions at heavy valence quark masses,

in general $m_h > m_{c0}$; we also fit the quark mass dependence of pseudoscalar masses with the linear form

$$M_{\eta_b} = d_h + b_h m_h. \quad (8)$$

With the experimental value of the η_b meson mass, the quark mass ratio can be evaluated as

$$\begin{aligned} \frac{m_b}{m_c} &= \frac{M_{\eta_b} - d_h}{\bar{M} - d} \frac{b}{b_h} \\ &= \frac{b}{b_h} \frac{r_1 M_{\eta_b} - d_{h0}(r_1/a)}{r_1 \bar{M} - d_0(r_1/a)}, \end{aligned} \quad (9)$$

where $d_{h0} = ad_h$. Here, we use the pseudoscalar mass instead of the spin averaged mass because the effects of hyperfine splitting are quite small compared to the overall mass scale. Even in the state-of-the-art lattice simulations, it is difficult to obtain the η_b mass because $am_b \sim 1.0$, and the discretization errors are significant. To circumvent this problem, we perform calculations for several values of the valence quark masses that are smaller than the bottom quark mass and extrapolate to the region of the bottom quark mass. If the utilized valence quark masses are too small, this procedure could have systematic uncertainties. To investigate such uncertainties, we perform the extrapolations from the data points at $am_h < 1.0$ to m_{b0} with several mass ranges and estimate discrepancy between the results obtained using different ranges. These discrepancies are treated as systematic errors.

Once the lattice charm quark masses m_{c0} corresponding to the physical value have been determined, we calculate the pseudoscalar charmonium correlator with the valence mass of m_{c0} using point sources. Then, we consider the moments of the pseudoscalar charmonium correlator, which are defined as

$$G_n = \sum_t t^n G(t), \quad G(t) = a^6 \sum_{\mathbf{x}} (am_{c0})^2 \langle j_5(\mathbf{x}, t) j_5(0, 0) \rangle, \quad (10)$$

Here, $j_5 = \bar{\psi} \gamma_5 \psi$ is the pseudoscalar current. To take into account the periodicity of the lattice of temporal size N_t , the above definition of the moments can be generalized as follows:

$$G_n = \sum_t t^n (G(t) + G(N_t - t)). \quad (11)$$

The moments G_n are finite for $n \geq 4$ (n even) since the correlation function diverges as t^{-4} for small t . Furthermore, the moments G_n do not need renormalization because the explicit factors of the quark mass are included in their definition [28]. They can be calculated in perturbation theory in $\overline{\text{MS}}$ scheme

$$G_n = \frac{g_n(\alpha_s(\mu), \mu/m_c)}{am_c^{n-4}(\mu)}. \quad (12)$$

Here, μ is the $\overline{\text{MS}}$ renormalization scale. The coefficient $g_n(\alpha_s(\mu), \mu/m_c)$ is calculated up to 4-loop, i.e., up to order α_s^3 [29–31]. Given the lattice data on G_n , one can extract $\alpha_s(\mu)$ and $m_c(\mu)$ from the above equation. However, as it was pointed out in Ref. [28], it is more practical to consider the reduced moments

$$R_n = \begin{cases} G_n/G_n^{(0)} & (n = 4) \\ (G_n/G_n^{(0)})^{1/(n-4)} & (n \geq 6) \end{cases}, \quad (13)$$

TABLE I: The gauge couplings (β), lattice sizes ($N_s^3 \times N_t$), and the strange quark masses (am_s) used in our calculations, as well as corresponding lattice spacing (a^{-1} [GeV]). The number of trajectories (traj.) we use to calculate the charmonium correlation function with the corner-wall sources are also summarized, as well as the results for the bare charm quark masses, m_{c0} in GeV, and ratios of charm to strange quark masses (m_c/m_s). The calculations have been done every five trajectories for $N_t = 32$ and 48 and six trajectories for $N_t = 64$.

β	$N_s^3 \times N_t$	am_s	a^{-1} [GeV]	traj.	m_{c0}	m_c/m_s
6.488	32^4	0.0620	1.42	2500	1.0899(23)	12.586(28)
6.515	32^4	0.0604	1.46	2500	1.0810(23)	12.518(28)
6.664	32^4	0.0514	1.69	2500	1.0407(20)	12.299(25)
6.740	48^4	0.0476	1.81	2440	1.0215(18)	12.162(22)
6.880	48^4	0.0412	2.07	2465	0.9935(21)	12.023(26)
7.030	48^4	0.0356	2.39	1530	0.9673(21)	11.917(27)
7.150	$48^3 \times 64$	0.0320	2.67	2406	0.9471(25)	11.926(32)
7.280	$48^3 \times 64$	0.0284	3.01	2376	0.9289(25)	11.886(34)
7.373	$48^3 \times 64$	0.0250	3.28	1206	0.9161(27)	11.832(35)
7.596	64^4	0.0202	4.00	1200	0.8878(34)	11.850(46)
7.825	64^4	0.0164	4.89	1200	0.8679(57)	11.930(80)

where $G_n^{(0)}$ is the moment calculated from the free correlation function. The lattice artifacts largely cancel out in these reduced moments. It is straightforward to write down the perturbative expansion for R_n :

$$R_n = \begin{cases} r_4 & (n = 4) \\ r_n \cdot (m_{c0}/m_c(\mu)) & (n \geq 6) \end{cases}, \quad (14)$$

$$r_n = 1 + \sum_{j=1}^3 r_{nj}(\mu, m_c) \alpha_s^j(\mu). \quad (15)$$

For the choice of the renormalization scale $\mu = m_c$, the expansion coefficients are just simple numbers that have been tabulated, for example, in Ref. [11]. This choice of the renormalization scale has the advantage that the expansion coefficients are never large.

III. NUMERICAL ANALYSIS AND CONTINUUM EXTRAPOLATIONS

A. Determinations of m_{c0} and ratios m_c/m_s and m_b/m_c

To obtain the value of m_{c0} as well as m_c/m_s and m_b/m_c at each lattice spacing, we need physical masses: \bar{M} , $M_{\eta_{ss}}$, and M_{η_b} . We directly utilize the experimental value $M_{\eta_b} = 9.3980(32)$ GeV from PDG [5], whereas to specify \bar{M} we take the values of η_c and J/ψ masses from PDG and obtain $\bar{M} = 3.067$ GeV.

The gauge configurations used in our study are summarized in Table I, together with the number of analyzed trajectories and the corresponding lattice spacings. The statistical errors on meson masses and more generally on meson correlation functions and their moments have been estimated using jackknife analysis. We varied the jackknife bin size and checked

that the estimated statistical errors do not change significantly. Therefore, the analysis does not suffer from the effects of autocorrelations.

Our calculation neglects disconnected diagrams and electromagnetic effects. The effect of disconnected diagrams on the ground state charmonium is known to be a few MeV [32]. Electromagnetic effects are of similar size [11]. Therefore, following Ref. [11], we assign an error of 3 MeV to the value of \overline{M} . On the other hand, to estimate the unmixed pseudoscalar $s\bar{s}$ meson mass, we use the leading order chiral perturbation theory, $M_{\eta_{ss}} = \sqrt{2M_K^2 - M_\pi^2}$. We need, however, to take into account the breaking of the isospin symmetry and the electromagnetic effects, which are neglected in our calculations. Following Ref. [33] for the pion and kaon masses, we write

$$M_\pi^2 = M_{\pi^0}^2, \quad (16)$$

$$M_K^2 = \frac{1}{2}(M_{K^0}^2 + M_{K^+}^2 - (1 + \Delta_E)(M_{\pi^+}^2 - M_{\pi^0}^2)). \quad (17)$$

The parameter Δ_E characterizes the violation of the Dashen theorem stating that in the chiral limit the electromagnetic corrections to M_{K^+} and M_{π^+} are the same, while there are no electromagnetic corrections to M_{π^0} and M_{K^0} . The value of Δ_E was determined to be $\Delta_E = 0.84(25)$ [34]. There is also a very recent lattice determination of this parameter [35]. Here, however, we follow Ref. [33] and use a more conservative approach varying Δ_E from 0 to 2. We find

$$M_{\eta_{ss}} = 686.00(92) \text{ MeV}, \quad (18)$$

where the central value corresponds to $\Delta_E = 0$. This value is in excellent agreement with the HPQCD determination, $M_{\eta_{ss}} = 685.8(3.8)(1.2) \text{ MeV}$ [26], making us confident that the value based on leading order chiral perturbation theory is accurate.

To associate the absolute scale r_1 with evaluated quantities on the lattice, we use the values of r_1/a given in Table VIII of Ref. [21]. These values are obtained from the interpolation of the calculated r_1/a values [21]. Since r_1/a is a smooth function of the gauge coupling, the errors in the determination of r_1/a can be largely reduced by using a smooth interpolation (see Ref. [21] for details). We also performed the analysis using the calculated value of r_1/a at each β and checked that our final result does not change.

Now, we can determine the bare charm quark mass m_{c0} on the lattice and the mass ratio of the charm to strange quarks. To determine d_0 and b at each β , we calculate the masses of J/ψ and η_c mesons for several trial values of the charm quark mass in the range that encompasses the physical value of the charm quark mass. Some details on the determination of the charmonium masses are given in the Appendix. We perform interpolation of the calculated spin averaged mass \overline{M} to its physical value. We find that the linear fits $a\overline{M} = d_0 + b(am_{ci})$ work very well, and the statistical errors of d_0 and b are estimated using the bootstrap analysis. The results of m_{c0} are also shown in Table I with the number of trajectories used to calculate J/ψ and η_c masses. The statistical errors on m_{c0} are

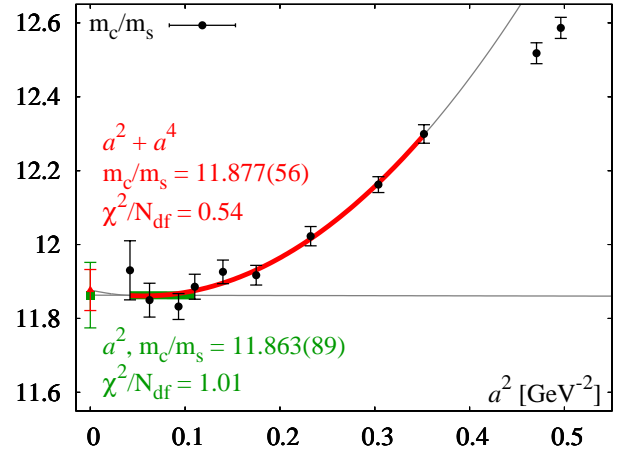


FIG. 1: The lattice spacing dependence of m_c/m_s together with continuum extrapolations. The triangle (square) corresponds to the a^2 ($a^2 + a^4$) continuum extrapolation. The results of extrapolations with χ^2/N_{df} of the fits are also shown. The thick lines show the extrapolation curves in the interval in which the fits have been performed, while the thin lines show the same curves outside that interval.

estimated from the errors on d_0 and b , as well as from the errors on r_1/a added in quadrature. Table I shows that the determination of m_{c0} achieves an accuracy of 0.4%, except for the highest β value, where the error becomes about 0.7% mainly due to the uncertainty of r_1/a . The determined m_{c0} values are used for the calculations of the moments of the pseudoscalar charmonium correlator discussed below.

Using the value of B_0 calculated from the values of am_s and $aM_{\eta_{ss}}$ given in Tables III and V of Ref. [21], $B_0 = (aM_{\eta_{ss}})^2/am_s$, and we can determine m_c/m_s using Eq. (7) at each lattice spacing. The error on B_0 comes from the error on the mass of the unmixed pseudoscalar $s\bar{s}$ meson determined in Ref. [21]. This error was included in the analysis, however, it is subdominant. The results are shown in Fig. 1 as a function of a^2 . At this point, we do not include the errors on \overline{M} , $M_{\eta_{ss}}$, and the physical value of r_1 , as these are common for all data points. We performed continuum extrapolations using the a^2 form as well as the a^2 form plus a^4 term. These are shown in Fig. 1. The coarsest two lattice spacings are not in the scaling regime and therefore are not included in the final analysis. Using $a^2 + a^4$ extrapolation we obtain $m_c/m_s = 11.877(56)$ with $\chi^2/N_{\text{df}} = 0.54$, while for the a^2 extrapolation we have $11.863(89)$ with $\chi^2/N_{\text{df}} = 1.01$. Since the two extrapolations agree within the errors, we take $m_c/m_s = 11.877(56)$ as our final continuum result. Now, adding the errors from the absolute values of \overline{M} , $M_{\eta_{ss}}$, and r_1 we obtain our final result:

$$\frac{m_c}{m_s} = 11.877(56)(72), \quad (19)$$

where the first (second) parenthesis indicates the statistical (scale) uncertainty.

To test possible cutoff effects in our calculations, we consider the charmonium spectra and hyperfine splitting in the continuum limit. For the pseudoscalar (PS) and vector (V)

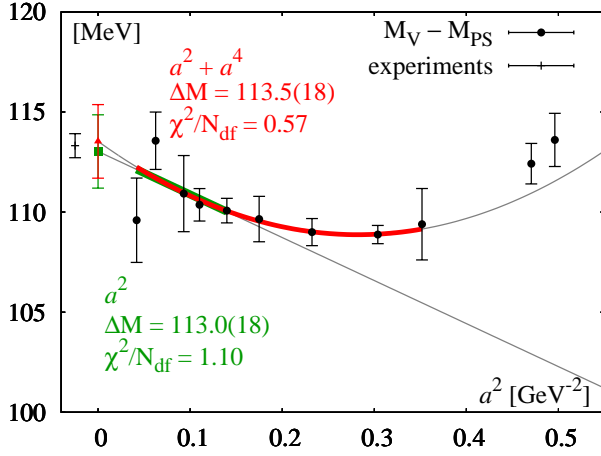


FIG. 2: The lattice spacing dependence of the charmonium hyperfine splitting together with continuum extrapolations. The triangle (square) plot corresponds to the a^2 ($a^2 + a^4$) continuum extrapolation. The results of extrapolations with χ^2/N_{df} of the fits as well as the experimental value $M_{J/\psi} - M_{\eta_c} = 113.3(6)$ MeV are also shown. The thick lines show the extrapolation curves in the interval in which the fits have been performed, while the thin lines show the same curves outside that interval.

masses with the trial am_c values, we perform similar fits with Eq. (4) and obtain $d_0^{(i)}$ and $b^{(i)}$ with $i = \text{PS}$ and V . Then, those masses on the lattice can be determined as

$$M_i = r_1^{-1} \left(\frac{r_1}{a} \right) d_0^{(i)} + b^{(i)} m_{c0}, \quad i = \text{PS and V}. \quad (20)$$

We find that the dependence of the masses on the lattice spacing becomes very mild. From the continuum extrapolation using the a^2 form and the six highest β values, we obtain

$$M_{\text{PS}} = 2.982(12) \text{ GeV}, \quad (21)$$

$$M_{\text{V}} = 3.095(12) \text{ GeV}, \quad (22)$$

which agree well with the experimental values $M_{\eta_c} = 2.9836(6)$ GeV and $M_{J/\psi} = 3.096916(11)$ GeV. The hyperfine splitting $\Delta M \equiv M_{\text{V}} - M_{\text{PS}}$ can also be extracted from the lattice masses and is shown in Fig. 2. We perform continuum extrapolations of the hyperfine splitting using a^2 and $a^2 + a^4$ forms, which are also shown in Fig. 2. The results from the two continuum extrapolations agree very well within the errors. Taking the results from the $a^2 + a^4$ extrapolations and considering the errors from the absolute values of \bar{M} and r_1 , we obtain:

$$\Delta M = 113.5(18)(7) \text{ MeV}. \quad (23)$$

This agrees very well with the experimental value $M_{J/\psi} - M_{\eta_c} = 113.3(6)$ MeV.

In the end of the subsection, we determine the ratio of the bottom to charm quark mass m_b/m_c . For this purpose, we chose heavier valence masses than the charm quark mass, $m_h > m_{c0}$, and calculate the pseudoscalar meson mass M_{η_b} . For the four finest lattice spacings at $\beta = 7.280\text{--}7.825$, we

calculate the meson correlation functions at $0.5 \leq am_h \leq 1.0$ and determine the quark mass dependence of M_{η_b} according to Eq. (8). The number of trajectories we use for this calculation is summarized in Table II for each gauge coupling β . The details of the extraction of the heavy pseudoscalar meson masses are discussed in the Appendix. The parameters d_{h0} and b_h are determined by the linear fittings of M_{η_b} as a function of m_h , with three data at $am_h = 0.7, 0.8$ and 0.9 . In our calculations, the interpolation from M_{η_b} to the experimental M_{η_b} is possible for $\beta = 7.825$. For other β values, however, the bottom quark mass corresponds to the region $am_h > 1$, and extrapolations are necessary to obtain M_{η_b} . We estimate uncertainties coming from the extrapolation to the bottom quark masses in the following way: First, by using d_{h0} and b_h obtained from the fit at $am_h = (0.7, 0.8, 0.9)$, we determine the bare bottom quark mass m_{b0} at each β as

$$m_{b0} = \frac{1}{b_h} \left[M_{\eta_b} - d_{h0} \left(\frac{r_1}{a} \right) r_1^{-1} \right]. \quad (24)$$

Then, we iterate the fit with the different data points at $0.5 \leq am_h \leq 1.0$, e.g., $am_h = (0.8, 0.9, 1.0)$, and calculate m_{b0} again. The difference between these two values provides an estimate of the systematic errors. The numerical values of m_b/m_c obtained from Eq. (9) are summarized in Table II, where the first and second parentheses indicate the statistical and systematic errors, respectively. The lattice spacing dependence of m_b/m_c is shown in Fig. 3, where the error bars and gray shadows indicate the statistical and systematic errors, respectively. We find that the lattice spacing dependence is very mild. The systematic errors become larger on coarser lattices and are significantly larger than the statistical errors for $\beta \leq 7.373$. Although there is no significant lattice spacing dependence, we perform the continuum extrapolations with the a^2 form, including the uncertainties from the statistical and systematic errors in quadrature. As a consequence we obtain

$$\frac{m_b}{m_c} = 4.528(50)(27), \quad (25)$$

where the number in the first parenthesis shows the combined statistical and extrapolation errors, and the number in the second parenthesis is the combined error from the values of \bar{M} , M_{η_b} and r_1 . As a test of our approach, we have performed the calculations of m_b/m_c by using vector bottomonium M_{V} masses obtained on the lattice combined with the experimental Υ mass and obtained the value $m_b/m_c = 4.531(52)$, which is essentially the same as above. The small lattice spacing dependence of the ratio m_b/m_c may appear somewhat surprising. Note, however, that the discretization errors for the HISQ action are small also in the heavy quark mass region as long as $am_h \leq 1$ [20]. In particular, the cutoff dependence of the ground state quarkonium masses was studied in a wide range of quark masses and was found to be small [17]. This is the reason why the cutoff dependence of m_b/m_c is small.

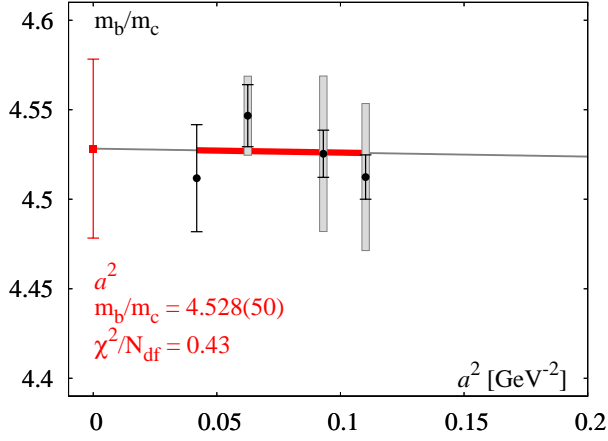


FIG. 3: The lattice spacing dependence of m_b/m_c . The error bars indicate the statistical errors, whereas the gray shadows indicate systematic uncertainties due to the heavy quark mass extrapolations (see text for more details). Result of the continuum extrapolation done by the a^2 form is also shown with χ^2/N_{df} value of the fit. The thick line shows the extrapolation curve in the interval in which the fit has been performed, while the thin line shows the same curve outside that interval.

TABLE II: The gauge coupling (β) and the number of trajectories (traj.) used to calculate the bottomonium correlation functions with the corner-wall sources. Also shown are the results of the ratios of the bottom to charm quark mass. The first parenthesis in the last column indicates the statistical errors, and the second one indicates the systematic errors due to extrapolations to heavy quark masses (see the text for more detail).

β	traj.	m_b/m_c
7.280	1800	4.512(12)(41)
7.373	1800	4.525(13)(43)
7.596	1680	4.547(17)(22)
7.825	2562	4.512(30)(0)

B. Strong coupling constant and quark masses from the moments

The strong coupling constant is determined from the moments of the pseudoscalar charmonium correlators on the lattice combined with the perturbative expansion of the corresponding quantity. We calculate the pseudoscalar charmonium meson correlators with the valence mass m_{c0} determined above using point sources with large statistics. Gauge couplings β and the number of trajectories used to calculate the moments are summarized in Table III (see also Table I for the corresponding lattice size and m_{c0}). The numerical results of the reduced moments are also summarized in Table III up to $n \leq 10$. The statistical errors of the reduced moments R_n have been estimated using jackknife procedure, and we checked again that there is no dependence on the jackknife bin size.

Since the lattice gauge configurations used in our study do not include the effects of charm quarks, following Ref. [28]

we estimate such effects using perturbation theory. It was shown that charm quarks increase the value of R_4 by 0.7% [28]. Therefore, we scale our lattice results for R_4 by 1.007. In the following, we always give the rescaled value of R_4 . The results of R_4 are shown in Fig. 4 as a function of the lattice spacing a^2 . The lattice spacing dependence of R_4 is significant, and for the coarsest lattice, it amounts to 6%. We have performed continuum extrapolation of our results using various fit forms. For HISQ action, the leading discretization effects are expected to be $\alpha_s a^2$ and a^4 . It is usually assumed that the running of the coupling constant α_s can be neglected if the considered range of the lattice spacing is not too large. Therefore, we can fit the numerical results for R_4 using a^2 and $a^2 + a^4$ forms. We could also perform continuum extrapolations using the $\alpha_s a^2$ form by defining the boosted coupling constant

$$\alpha_s^b(1/a) = \frac{1}{4\pi} \frac{g_0^2}{u_0^2}, \quad (26)$$

where $g_0^2 = 10/\beta$ is a bare lattice gauge coupling and u_0 is an averaged link valuable defined by the plaquette $u_0^4 = \langle \text{Tr} U_{\square} \rangle / 3$. Furthermore, we perform continuum extrapolations using $\alpha_s a^2 + a^4$ and $\alpha_s^b(a^2 + a^4)$ forms. We obtain the following continuum results:

$$\begin{aligned} R_4 &= 1.2743(40), \quad a^2 \text{ fit} \\ R_4 &= 1.2799(53), \quad a^2 + a^4 \text{ fit} \\ R_4 &= 1.2705(37), \quad \alpha_s^b a^2 \text{ fit} \\ R_4 &= 1.2769(49), \quad \alpha_s^b a^2 + a^4 \text{ fit} \\ R_4 &= 1.2759(47), \quad \alpha_s^b(a^2 + a^4) \text{ fit} \end{aligned} \quad (27)$$

The continuum extrapolations with a^2 and $a^2 + a^4$ forms are shown in Fig. 4. When performing fits with a^2 and $\alpha_s^b a^2$ forms, the data for the two coarsest lattice spacings have been excluded since these are not in the scaling regime. As our final continuum result, we take the value of R_4 obtained from the simple a^2 extrapolation and assign a systematic error of 0.0047 due to the continuum extrapolation to take into account the spread in the central values of R_4 obtained above:

$$R_4 = 1.2743(40)(47). \quad (28)$$

Our continuum result for R_4 agrees with the continuum results $R_4 = 1.281(5)$ and $R_4 = 1.282(4)$ obtained in Ref. [28] and Ref. [17], respectively, within errors. Our central value is slightly smaller. It should be pointed out that we have many more lattice spacings in the region $a < 0.1$ fm to perform the continuum extrapolations compared to Refs. [28] and [17].

Using the above results for R_4 as well as the corresponding perturbative expansion, it is straightforward to determine $\alpha_s(\mu = m_c)$. We obtain the value

$$\alpha_s(\mu = m_c, n_f = 3) = 0.3697(54)(64)(15), \quad (29)$$

where the first error is statistical, the second error corresponds to the uncertainty of the continuum extrapolation, and the last error comes from the truncation of the perturbative series for r_4 . The truncation error was estimated as follows: First, we

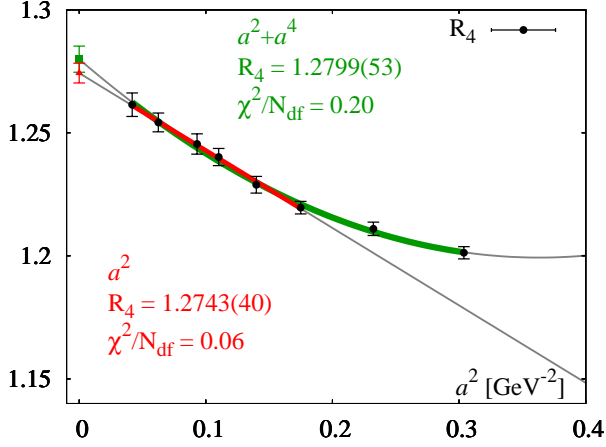


FIG. 4: Lattice results for R_4 . Also shown are the continuum extrapolations. The thick lines show the extrapolation curves in the interval in which the fits have been performed, while the thin lines show the same curves outside that interval.

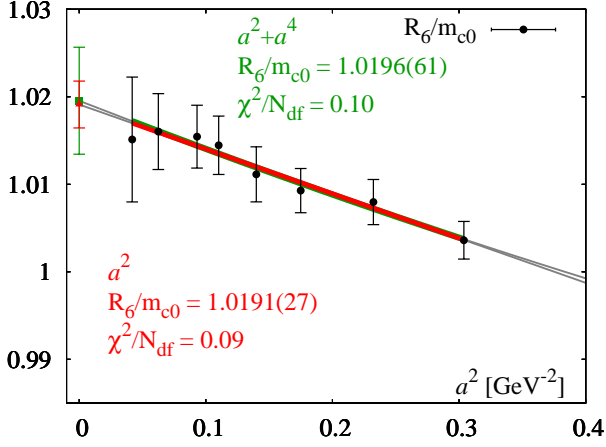


FIG. 5: Lattice results for R_6 . Also shown are the continuum extrapolations. The thick lines show the extrapolation curves in the interval in which the fits have been performed, while the thin lines show the same curves outside that interval.

used the perturbative result up to order α_s^3 to estimate the strong coupling constant. Then we included α_s^4 term with a coefficient equal to $r_{43} \times 2$ and estimated the strong coupling constant again. The difference between these two estimates is the truncation error.

Now let us discuss the determination of the charm quark mass. The value of the charm quark mass is also needed to specify α_s at any scale using Eq. (29). We determine the charm quark mass by considering R_6 . The $\overline{\text{MS}}$ charm mass can be estimated from the lattice mass as $m_c = r_6/(R_6/m_{c0})$. The effect of charm quark loops turns out to be much smaller for R_6 than for R_4 when estimated using perturbation theory. It was estimated that charm quark loops increase R_6 and this effect amounts to 0.1% [28]. We corrected our lattice data for this tiny effect and always show the corrected values of R_6

in the discussions below. Our lattice results for R_6/m_{c0} are shown in Fig. 5. The lattice spacing dependence of R_6/m_{c0} is milder than for R_4 . The maximal discretization errors are less than 2%. This is not surprising since the contribution to G_6 from the data points at small t is smaller than for G_4 . The data points at small t are the most sensitive to the lattice artifacts.

To obtain the continuum result, we again perform a^2 extrapolation which results in $R_6/m_{c0} = 1.0191(27)$. Performing an extrapolation with the a^4 term included results in $R_6/m_{c0} = 1.0196(61)$, which is in very good agreement with the above result (shown in Fig. 5). We also performed extrapolations using $\alpha_s a^2$ and $\alpha_s a^2 + a^4$ forms and obtained $R_6/m_{c0} = 1.0181(23)$ and $R_6/m_{c0} = 1.0192(56)$, respectively. Since all the above continuum results agree well within the estimated statistical errors, we use the value from simple a^2 extrapolations as our final continuum estimate

$$R_6/m_{c0} = 1.0191(27). \quad (30)$$

Using this and the perturbative result for r_6 , we obtain

$$m_c(\mu = m_c, n_f = 3) = 1.2668(33)(34)(79)(73) \text{ GeV}, \quad (31)$$

where the first error is statistical, the second error is the truncation error in r_6 , the third error comes from α_s determined above, and the last error comes from setting the scale in our lattice calculations.

The higher moments can also be utilized to determine α_s and m_c . Namely, we can use R_{n-2}/R_n to determine α_s and R_n/m_{c0} to determine $m_c(m_c)$. Here, $n \geq 8$. These calculations provide a valuable cross check for the extraction of α_s and m_c . There is also an advantage that the lattice spacing dependence for higher moments is expected to become milder as discussed above. Thus, more accurate continuum extrapolations could be possible. There is, however, a disadvantage in using higher moments. Higher order contributions in the perturbative expansion become significant for higher moments, but the perturbative coefficients are known up to α_s^3 orders at present. The absence of higher order perturbative calculations leads to larger truncation errors. On the lattice side there is also a disadvantage that the higher moments require information of the correlation functions at larger distance [c.f. Eq. (11)], but the calculation is performed on the finite lattice. Thus, the results for the higher moments potentially suffer from larger finite volume effects. In our calculations, the finite volume effects become more serious at finer lattice spacing.

In our study, the finite volume effects mostly appear in the moments of the free correlation functions $G_n^{(0)}$ introduced in Eq. (13). This is due to the fact that the exponential decay of the free meson correlator is governed by $2m_{c0} \approx 1.8 - 2.0 \text{ GeV}$ rather than by $m_{\eta_c} \approx 3 \text{ GeV}$. To investigate such effects, we calculate the free moments in the infinite temporal-size limit by using the results of $1.5N_t$ and $2N_t$ and estimate the finite volume effects from $G_n^{(0)}(N_t)/G_n^{(0)}(\infty)$, where the numerator is the same one used in Eq. (13), whereas the denominator is that on the infinite temporal size. We perform this calculation for the highest two β values and find that the effects become negligible for $n \leq 6$, whereas 1% and 6% effects appear for R_8 and R_{10} at $\beta = 7.596$, respectively, and 7% and 23% effects appear

TABLE III: The gauge couplings (β) and the number of trajectories (traj.) used for the calculations of the moments of the pseudoscalar correlation functions with the valence mass m_{c0} and point sources. Numerical results of the reduced moments R_n are also shown up to $n \leq 10$.

β	traj.	R_4	R_6	R_8	R_{10}
6.740	8005	1.2012(24)	1.0252(12)	0.94261(67)	0.89873(48)
6.880	8095	1.2110(27)	1.0014(13)	0.91399(75)	0.87025(54)
7.030	9830	1.2196(25)	0.9763(12)	0.88726(69)	0.84523(50)
7.150	7902	1.2289(33)	0.9577(16)	0.86794(83)	0.82661(58)
7.280	8058	1.2401(34)	0.9424(17)	0.85182(90)	0.81119(63)
7.373	9246	1.2454(41)	0.9303(18)	0.84022(94)	0.80054(65)
7.596	9510	1.2542(38)	0.9020(17)	—	—
7.825	9516	1.2614(47)	0.8811(20)	—	—

for R_8 and R_{10} at $\beta = 7.825$, respectively. Those are larger than the amount of the statistical errors of corresponding quantities and we omit the corresponding data in our analysis. We perform the continuum extrapolations of R_{n-2}/R_n and R_n/m_{c0} for $n = 8$ and 10 using a^2 form and including the lattice data for $\beta = 7.030$ – 7.373 and obtain the following continuum results:

$$R_6/R_8 = 1.1140(18), \quad (32)$$

$$R_8/R_{10} = 1.04954(65), \quad (33)$$

$$R_8/m_{c0} = 0.9167(54), \quad (34)$$

$$R_{10}/m_{c0} = 0.8731(50). \quad (35)$$

Since the continuum extrapolations using the $a^2 + a^4$ fit form with the lattice data for $\beta = 6.740$ – 7.373 leads to results that agree very well with the above results within errors, we consider them as our final continuum results. From the continuum results for the ratio R_{n-2}/R_n and R_n/m_{c0} , we obtain the following values for α_s and m_c :

$$\begin{array}{ll} n = 8 & n = 10 \\ \alpha_s(m_c) = 0.3954(71)(210) & 0.3611(50)(152) \\ m_c(m_c) = 1.2717(75)(9) & 1.2708(73)(35), \end{array} \quad (36)$$

where the first (second) parenthesis indicates the statistical (truncation) errors. We see that the truncation errors for α_s are an order of magnitude larger than the truncation errors coming from R_4 . Within the large errors, the above values of α_s are consistent with the α_s determination from the fourth moment. On the other hand, the truncation errors are fairly small for the charm quark mass, and the above values of m_c agree well with our previous determination.

Before concluding this section, let us compare the continuum results for the higher moments R_n , $n \geq 6$ with the HPQCD results [17, 28]. In Refs. [17, 28] a slightly different definition of R_n was used: $R_n = m_{\eta_c}/(2m_{c0})(G_n/G_n^{(0)})^{1/(n-4)}$. If we use this definition, we obtain $R_6 = 1.520(4)$, $R_8 = 1.367(8)$, and $R_{10} = 1.302(8)$, which agree well with the results of Ref. [17]: $R_6 = 1.527(4)$, $R_8 = 1.373(3)$, and $R_{10} = 1.304(2)$, as well as with the results of Ref. [28]: $R_6 = 1.528(11)$, $R_8 = 1.370(10)$, and $R_{10} = 1.304(9)$.

IV. SUMMARY OF RESULTS AND COMPARISON WITH OTHER WORKS

Now, we summarize the main findings of this paper. From the masses of pseudoscalar and vector mesons on the lattice we obtained the quark mass ratios:

$$\frac{m_c}{m_s} = 11.877(91), \quad \frac{m_b}{m_c} = 4.528(57), \quad (37)$$

where the statistical and systematic errors are added in quadrature. On the other hand, from the moments of the pseudoscalar charmonium correlation functions, we estimated the strong coupling constant and the charm quark masses in $\overline{\text{MS}}$ scheme for $\mu = m_c$:

$$\alpha_s(\mu = m_c, n_f = 3) = 0.3697(85), \quad (38)$$

$$m_c(\mu = m_c, n_f = 3) = 1.267(12) \text{ GeV}. \quad (39)$$

Let us first compare the quark mass ratios, which are scale and scheme independent quantities, with other lattice determinations. In Fig. 6, we show our result on m_c/m_s and compare it with several recent lattice QCD results. We find that the results in 2+1 flavor simulations show similar values. Our result for m_c/m_s is about one sigma larger than 2+1+1 flavor results. In Fig. 7, we compare our result on m_b/m_c with other recent lattice QCD determinations. Our result agrees well with the result from the HPQCD Collaboration and has similar errors. By just multiplying both ratios, we obtain the mass ratio of the bottom to the strange quarks:

$$\frac{m_b}{m_s} = 53.78(79). \quad (40)$$

This can be compared with one of the prediction in the grand unified theory, namely, the Georgi-Jarlskog relation which states: $m_b/m_s = 3m_\tau/m_\mu = 50.45$ [36]. Our result is 6% away from this prediction.

To compare our result on the strong coupling constant with other determinations, we need to evolve it to higher scales μ . We do so by using the 4-loop perturbation theory in the $\overline{\text{MS}}$ scheme and the RunDeC package [37]. First, we compare our result to two low energy determinations of α_s in 2+1 flavor lattice QCD simulations. One of them comes from the analysis of static quark-antiquark energy [3, 4] with the most recent value $\alpha_s(1.5 \text{ GeV}) = 0.336(+12)(-0.008)$ [4]. Evolving our result to $\mu = 1.5 \text{ GeV}$ and propagating the uncertainties, we obtain

$$\alpha_s(1.5 \text{ GeV}, n_f = 3) = 0.3316(69) \quad (41)$$

in excellent agreement with the above result. Another low energy determination of α_s by the HPQCD Collaboration comes from the lattice calculations of the moments of meson correlators consisting of heavy quarks with several values of the heavy quark mass and the Bayesian fit of these correlators to the perturbative result [17]: $\alpha_s(5 \text{ GeV}, n_f = 3) = 0.2034(21)$. Evolving our results to $\mu = 5 \text{ GeV}$ and propagating the errors, we obtain

$$\alpha_s(5 \text{ GeV}, n_f = 3) = 0.1978(22), \quad (42)$$

which is two sigma lower than the above result. Furthermore, we evolve our result to the commonly used scale $\mu = M_Z$ with $n_f = 5$ by adding the contributions of the charm and bottom quarks using the RunDeC package¹

$$\alpha_s(M_Z, n_f = 5) = 0.11622(84). \quad (43)$$

In Fig. 8, we compare our $\alpha_s(M_Z)$ with recent results obtained by other collaborations. We see that our result is in agreement with Ref. [4] (“Bazavov’14”) but is lower than other lattice determinations.

The charm quark mass $m_c(m_c)$ was directly obtained by extrapolating the lattice moments to the continuum and matching those to the corresponding perturbative results. Figure 9 shows the comparison of our charm quark mass with the recent results of other collaborations. We find that our result is similar to other lattice determinations but is lower than the ETMC’14 result [12]. We can also calculate the strange and bottom quark masses from $m_c(m_c)$ with the quark mass ratios and obtain

$$m_s(\mu = 2 \text{ GeV}, n_f = 3) = 92.0(1.7) \text{ MeV}, \quad (44)$$

$$m_b(\mu = m_b, n_f = 5) = 4.184(89) \text{ GeV}. \quad (45)$$

Our result of $m_b(m_b)$ is almost the same as the recent result by the HPQCD Collaboration $m_b(m_b) = 4.162(48)$ [11] and also agrees with the ETMC result $m_b(m_b) = 4.26(10)$ [18] within the errors. On the other hand, for the strange quark mass, our result agrees well with the recent HPQCD result [11] within uncertainties: $m_s(2\text{GeV}) = 93.6(8) \text{ MeV}$. It is lower than the values obtained by the ETMC Collaboration [12], $m_s(2\text{GeV}) = 99.6(4.3) \text{ MeV}$ and Dürer *et al* [13], $m_s(2\text{GeV}) = 97.0(2.6)(2.5) \text{ MeV}$. Evolving our result to $\mu = 3 \text{ GeV}$, we get $m_s(3\text{GeV}) = 83.6(1.5)$. This is in good agreement with the result from RBC/UKQCD, $m_s(3\text{GeV}) = 81.64(1.17) \text{ MeV}$ [38].

V. CONCLUSION

We have performed determinations of the quark mass ratios as well as the strong coupling constant and the quark masses in 2+1 flavor lattice QCD simulations. The former have been obtained from the pseudoscalar and vector meson masses together with the experimental mass values, whereas the latter have been obtained from the moments of the pseudoscalar charmonium correlators and its comparison to the perturbative result at scale $\mu = m_c$.

At the level of the reduced moments our results agree well with the results obtained by the HPQCD Collaboration. Our results for bottom, charm and strange quark masses are also in very good agreement with the HPQCD results. We determined the QCD running coupling constant in the $\overline{\text{MS}}$ scheme

¹ In more detail, we start from our $\alpha_s(m_c, n_f = 3)$ and match it to $\alpha_s(m_c, n_f = 4)$ using $m_c(m_c)$ as the threshold. We evolve the corresponding $\alpha_s(m_c, n_f = 4)$ to the scale $\mu = m_b(m_b)$, where we match it to $\alpha_s(m_b, n_f = 5)$. Finally, we evolve the coupling constant to $\mu = M_Z$.

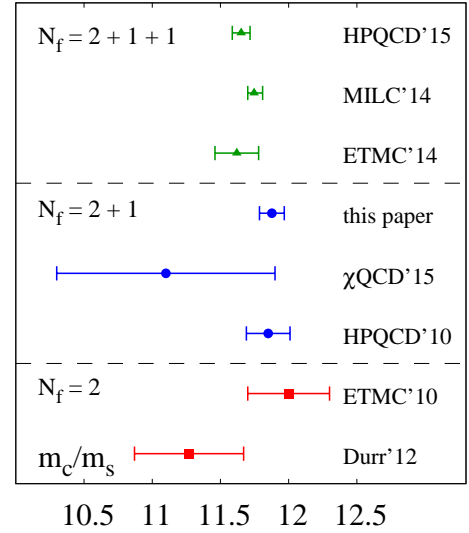


FIG. 6: Determinations of the ratio of the charm quark mass to strange quark mass m_c/m_s in lattice QCD simulations. We include the determinations from HPQCD’15 [11], MILC’14 [16], ETMC’14 [12], χ QCD’15 [15], HPQCD’10 [14], ETMC’10 [39], and Durr’12 [13].

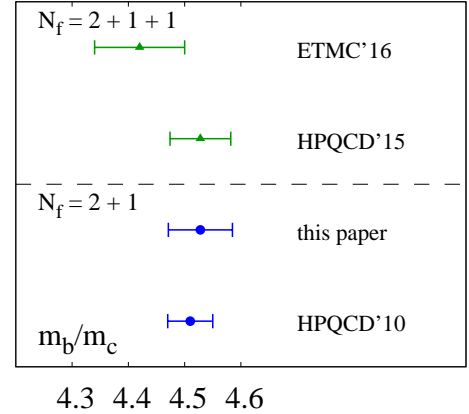


FIG. 7: Determinations of the ratio of the bottom quark mass to charm quark mass m_b/m_c in lattice QCD simulations. In the comparison we include the results from ETMC’16 [18], HPQCD’15 [11], and HPQCD’10 [17].

at the lowest energy scale so far. The error in our determination of the strong coupling constant is dominated by the lattice error, whereas the error due to the truncation of the perturbative series is very small. Evolving this low energy determination to $\mu = M_Z$ we obtain $\alpha_s(M_Z, n_f = 5) = 0.11622(84)$, which is lower than the most lattice QCD determinations, as well as the PDG value.

One open issue with the present determination based on moments of heavy meson correlators is whether the systematic error of the perturbative expansion is sufficiently conservative. Recent analysis seems to suggest that the error in the perturbative expansion may be underestimated [42].

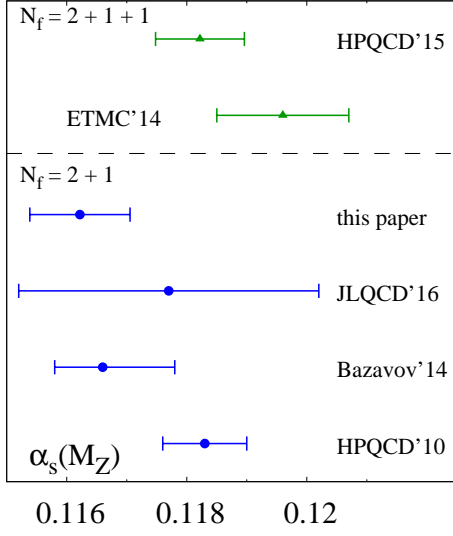


FIG. 8: Determinations of $\alpha_s(M_Z, n_f = 5)$ in lattice QCD simulations. Recent results are included from HPQCD'15 [11], ETMC'14 [40], JLQCD'16 [41], Bazavov'14 [4], and HPQCD'10 [14].

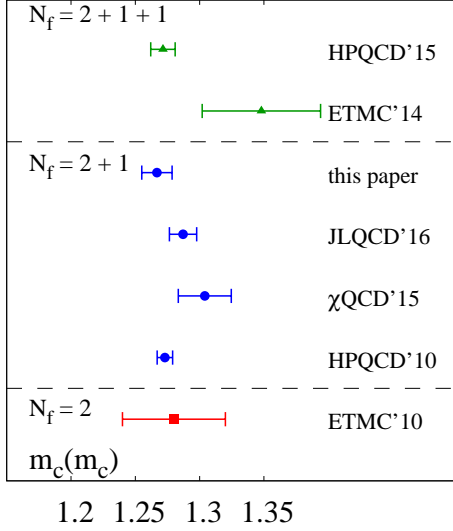


FIG. 9: Charm quark mass in $\overline{\text{MS}}$ scheme $m_c(\mu = m_c)$ obtained in this work and compared with other lattice determinations: HPQCD'15 [11], ETMC'14 [12], χ QCD'15 [15] HPQCD'10 [14], and ETMC'10 [39].

ACKNOWLEDGMENTS

This work was supported by U.S. Department of Energy under Contract No. de-sc0012704. The calculations have been carried out on USQCD clusters in Jlab. We thank Christian Hoebeling for useful discussions on the form of continuum extrapolations.

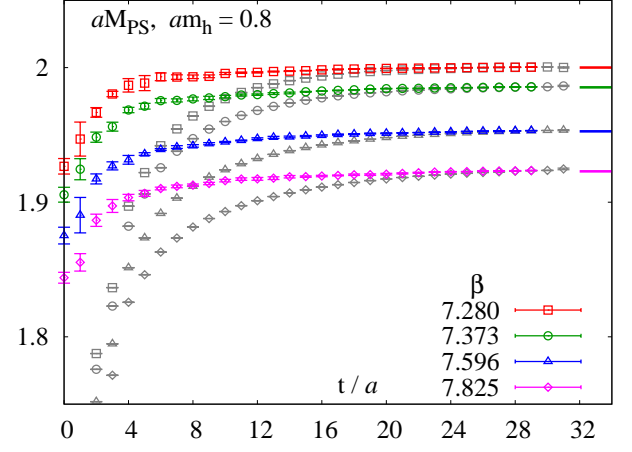


FIG. 10: Effective masses extracted from the pseudoscalar meson correlators at the valence quark mass of $am_h = 0.8$ (gray symbols) as a function of the separation t . Also shown are the extracted pseudoscalar meson masses as function of t_{\min}/a . The lines in the right-hand-side indicate estimated magnitude of the plateaus for each β (see text for more details).

Appendix A: Pseudoscalar meson masses

In this appendix, we discuss the determination of the pseudoscalar meson masses for various quark masses including the quark mass region utilized to estimate the bottom quark mass. To determine the bottom quark mass, we calculate the meson correlator in the pseudoscalar channel and estimate the lowest lying pseudoscalar meson masses, M_{η_h} , at the quark mass range of $0.7 \leq am_h \leq 0.9$. Then we extrapolate to the region of heavier quark masses. Thus, high quality extraction of the ground state meson masses is crucial to ensure the quality of the heavy quark extrapolations.

To demonstrate the quality of meson mass determination in Fig. 10, we show the effective masses as well as the fit results for the pseudoscalar channel at $am_h = 0.8$ obtained with corner-wall sources. In the figure, results for four β values are shown, which are used to estimate the bottom quark mass in the continuum limit. Here, the gray symbols correspond to the results of the effective masses, whereas the colored symbols depict the fit results of the pseudoscalar meson masses performed in the range at $[t_{\min}/a, N_t - t_{\min}/a]$. We find that both the effective masses and fit results approach a plateau for large t or large values of t_{\min}/a . On finer lattices, one needs larger separations to achieve the plateau. For the finest lattice, $\beta = 7.825$, the plateau behavior can be seen at $t/a \geq 24$. The values of the plateaus are estimated by averaging over the fit results $t_{\min}/a = 24-27$. This is also shown by the lines in the right-hand side. We find that the effective masses as well as the fit results are converged to the lines at a large distance which implies that magnitudes of our extracted plateau well reproduce the lowest lying masses of the corresponding states.

A similar analysis has been performed for the valence quark masses around the charm quark mass. The corresponding re-

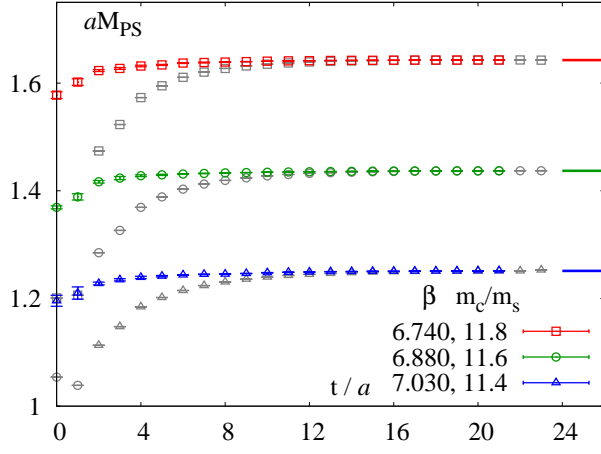


FIG. 11: Effective masses extracted from the pseudoscalar meson correlators with the valence quark masses around the charm quark mass (gray symbols) as a function of the separation t . Also shown are the extracted pseudoscalar meson masses as function of t_{\min}/a . The lines in the right-hand side indicate estimated values of the plateaus for each β (see text for more details).

sults are shown in Fig. 11 for several gauge couplings, β . Once again, we see that the extracted masses are stable with respect to the variation of t_{\min}/a within a reasonable range, and the extracted masses agree with the plateaus of the effective masses.

-
- [1] G. P. Lepage, P. B. Mackenzie, and M. E. Peskin (2014), 1404.0319.
 - [2] S. Moch et al. (2014), 1405.4781.
 - [3] A. Bazavov, N. Brambilla, X. Garcia i Tormo, P. Petreczky, J. Soto, and A. Vairo, Phys. Rev. **D86**, 114031 (2012), 1205.6155.
 - [4] A. Bazavov, N. Brambilla, X. Garcia i Tormo, P. Petreczky, J. Soto, and A. Vairo, Phys. Rev. **D90**, 074038 (2014), 1407.8437.
 - [5] K. A. Olive et al. (Particle Data Group), Chin. Phys. **C38**, 090001 (2014).
 - [6] A. Pich and A. Rodriguez-Sánchez (2016), 1605.06830.
 - [7] A. Bazavov, N. Brambilla, H. T. Ding, P. Petreczky, H. P. Schadler, A. Vairo, and J. H. Weber, Phys. Rev. **D93**, 114502 (2016), 1603.06637.
 - [8] M. Berwein, N. Brambilla, P. Petreczky, and A. Vairo, Phys. Rev. **D93**, 034010 (2016), 1512.08443.
 - [9] H. T. Ding, S. Mukherjee, H. Ohno, P. Petreczky, and H. P. Schadler, Phys. Rev. **D92**, 074043 (2015), 1507.06637.
 - [10] A. Bazavov, H. T. Ding, P. Hegde, F. Karsch, C. Miao, S. Mukherjee, P. Petreczky, C. Schmidt, and A. Velytsky, Phys. Rev. **D88**, 094021 (2013), 1309.2317.
 - [11] B. Chakraborty, C. T. H. Davies, B. Galloway, P. Knecht, J. Koponen, G. Donald, R. Dowdall, G. Lepage, and C. McNeile, Phys. Rev. **D91**, 054508 (2015), 1408.4169.
 - [12] N. Carrasco et al. (European Twisted Mass), Nucl. Phys. **B887**, 19 (2014), 1403.4504.
 - [13] S. Durr and G. Koutsou, Phys. Rev. Lett. **108**, 122003 (2012), 1108.1650.
 - [14] C. T. H. Davies, C. McNeile, K. Y. Wong, E. Follana, R. Horgan, K. Hornbostel, G. P. Lepage, J. Shigemitsu, and H. Trotter, Phys. Rev. Lett. **104**, 132003 (2010), 0910.3102.
 - [15] Y.-B. Yang et al., Phys. Rev. **D92**, 034517 (2015), 1410.3343.
 - [16] A. Bazavov et al. (Fermilab Lattice, MILC), Phys. Rev. **D90**, 074509 (2014), 1407.3772.
 - [17] C. McNeile, C. T. H. Davies, E. Follana, K. Hornbostel, and G. P. Lepage, Phys. Rev. **D82**, 034512 (2010), 1004.4285.
 - [18] A. Bussone et al. (ETM), Phys. Rev. **D93**, 114505 (2016), 1603.04306.
 - [19] M. Luscher and P. Weisz, Commun.Math.Phys. **97**, 59 (1985).
 - [20] E. Follana et al. (HPQCD Collaboration, UKQCD Collaboration), Phys. Rev. **D75**, 054502 (2007), hep-lat/0610092.
 - [21] A. Bazavov et al. (HotQCD), Phys. Rev. **D90**, 094503 (2014), 1407.6387.
 - [22] A. Bazavov, F. Karsch, Y. Maezawa, S. Mukherjee, and P. Petreczky, Phys. Rev. **D91**, 054503 (2015), 1411.3018.
 - [23] D. Mohler, A. S. Kronfeld, J. N. Simone, C. DeTar, S.-h. Lee, and L. Levkova (Fermilab Lattice, MILC), PoS **LATTICE2014**, 085 (2015), 1412.1057.
 - [24] A. Bazavov et al. (MILC Collaboration), PoS **LATTICE2010**, 074 (2010), 1012.0868.
 - [25] S. Borsanyi et al., JHEP **09**, 010 (2012), 1203.4469.
 - [26] C. T. H. Davies, E. Follana, I. D. Kendall, G. P. Lepage, and C. McNeile (HPQCD), Phys. Rev. **D81**, 034506 (2010), 0910.1229.
 - [27] G. P. Lepage, B. Clark, C. T. H. Davies, K. Hornbostel, P. B. Mackenzie, C. Morningstar, and H. Trotter, Nucl. Phys. Proc. Suppl. **106**, 12 (2002), [12(2001)], hep-lat/0110175.
 - [28] I. Allison et al. (HPQCD), Phys. Rev. **D78**, 054513 (2008), 0805.2999.
 - [29] C. Sturm, JHEP **09**, 075 (2008), 0805.3358.
 - [30] Y. Kiyo, A. Maier, P. Maierhofer, and P. Marquard, Nucl. Phys. **B823**, 269 (2009), 0907.2120.
 - [31] A. Maier, P. Maierhofer, P. Marquard, and A. V. Smirnov, Nucl. Phys. **B824**, 1 (2010), 0907.2117.
 - [32] L. Levkova and C. DeTar, Phys. Rev. **D83**, 074504 (2011), 1012.1837.
 - [33] C. Aubin, C. Bernard, C. E. DeTar, J. Osborn, S. Gottlieb, E. B. Gregory, D. Toussaint, U. M. Heller, J. E. Hetrick, and R. Sugar (MILC), Phys. Rev. **D70**, 114501 (2004), hep-lat/0407028.

- [34] J. Bijnens and J. Prades, Nucl. Phys. **B490**, 239 (1997), hep-ph/9610360.
- [35] Z. Fodor, C. Hoelbling, S. Krieg, L. Lellouch, T. Lippert, A. Portelli, A. Sastre, K. K. Szabo, and L. Varnhorst (2016), 1604.07112.
- [36] H. Georgi and C. Jarlskog, Phys. Lett. **B86**, 297 (1979).
- [37] K. G. Chetyrkin, J. H. Kuhn, and M. Steinhauser, Comput. Phys. Commun. **133**, 43 (2000), hep-ph/0004189.
- [38] T. Blum et al. (RBC, UKQCD), Phys. Rev. **D93**, 074505 (2016), 1411.7017.
- [39] B. Blossier, P. Dimopoulos, R. Frezzotti, V. Lubicz, M. Petschlies, F. Sanfilippo, S. Simula, and C. Tarantino (ETM), Phys. Rev. **D82**, 114513 (2010), 1010.3659.
- [40] B. Blossier, P. Boucaud, M. Brinet, F. De Soto, V. Morenas, O. Pene, K. Petrov, and J. Rodriguez-Quintero (ETM), Phys. Rev. **D89**, 014507 (2014), 1310.3763.
- [41] K. Nakayama, B. Fahy, and S. Hashimoto (2016), 1606.01002.
- [42] B. Dehnadi, A. H. Hoang, and V. Mateu, JHEP **08**, 155 (2015), 1504.07638.